Published in final edited form as:

ACS Biomater Sci Eng. 2019 December 09; 5(12): 6530–6540. doi:10.1021/acsbiomaterials.9b01289.

Model Particulate Drug Carriers Modulate Leukocyte Adhesion in Human Blood Flows

William J. Kelley[+], **Peter J. Onyskiw**[+], **Catherine A. Fromen**[+], **Omolola Eniola-Adefeso**[+,*]

[+]Department of Chemical Engineering, University of Michigan, Ann Arbor, MI 48109

Abstract

Drug carriers have been widely explored as a method of improving the efficacy of therapeutic drugs for a variety of diseases, including those involving inflammation. However, few of these formulations have advanced past clinical trials. There are still major gaps in our understanding of how drug carriers impact leukocytes, particularly in inflammatory conditions. In this work, we investigated how targeted and non-targeted drug carriers affect the function of leukocytes in blood flow. We explored three primary mechanisms: (1) collisions in blood flow disrupting leukocyte adhesion, (2) specific binding to the endothelium competes with leukocytes for binding sites, and (3) particle phagocytosis alters leukocyte phenotype, resulting in reduced adhesion. We find that each of these mechanisms contributes to significantly reduced leukocyte adhesion to an inflamed endothelium, and that particle phagocytosis may be the most significant driver of this effect. These results are crucial for understanding the totality of the impact of drug carriers on leukocyte behavior and response to inflammation and should inform the future design of any such drug carriers.

Graphical Abstract

Particulate drug carriers alter leukocyte adhesion to an inflamed endothelium *via* three primary mechanisms: nonspecific collisions in blood flow, specific blocking of leukocyte adhesion by occupying binding sites on the endothelium, and alterations in leukocyte phenotype after particle phagocytosis (left). Leukocyte adhesion to an inflamed endothelium *in vitro* under control (i.e., no particles) conditions, in the presence of 2 μm targeted particles, and 2 μm non-targeted particles (right).

[*]Corresponding author: lolaa@umich.edu.

Supporting Information

Supporting information containing the following accompanies this manuscript:

Microscope image showing co-localization of non-targeted nanoparticles with leukocytes (S1)

Figure plotting percent reduction in leukocyte adhesion versus particle adhesion (S2)

Figure plotting percent reduction in leukocyte adhesion versus surface coverage (S3)

Figure plotting percent reduction in leukocyte adhesion versus particle concentration for targeted and non-targeted particles (S4)

Figure plotting individual data points for percent reduction in leukocyte adhesion for 3 μm and 5 μm particles (S5)

Figure showing flow cytometry analysis of monocyte particle phagocytosis (S6)

Figure showing percentage of neutrophils in whole blood before and after PPFC experiments (S7)

Figure showing neutrophil rolling velocity and percent rolling versus firmly adherent neutrophils post-phagocytosis (S8).

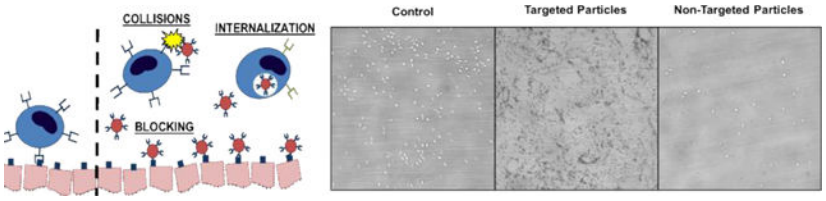

Keywords

drug delivery; vascular targeting; leukocyte adhesion; inflammation; neutrophils

Background

To date, a great deal of research has focused on the use of particulate carriers for the delivery of drugs to increase their efficacy while decreasing systemic side effects.[1,2] However, very few formulations have emerged from clinical trials and made it onto the market, likely due to inefficient targeting schemes, poor drug release kinetics, and possible mismatches between performance in artificial *in vitro* and *in vivo* experiments and clinical applications.[3–5] Indeed, despite the decades of research into polymeric particulate drug carriers, all of the drug delivery formulations approved to date are liposomal formulations except for Abraxane, an albumin-based particle formulation for the delivery of paclitaxel.[6] Notably, among the very few polymeric particulate drug carrier formulations to have reached Phase II/III clinical trials, none have convincingly demonstrated increased therapeutic benefit over free drug. For example, NK105, a polymeric micellar formulation of paclitaxel, showed no increased therapeutic benefit over paclitaxel alone in phase III clinical trial at a dose of 65 mg/m^2 (~1.8 mg/kg), and higher doses resulted in complications due to neutropenia.[7] Additionally, relatively little work has explored the impacts of particle drug carriers on leukocyte function in response to inflammation in blood flow, which is crucial to fully understand the efficacy and potential side effects of vascular-targeted drug carriers.

Typically, in an inflammatory event (e.g., vascular injury), the endothelial cells (ECs) lining the lumen of the blood vessel begin releasing cytokines (such as IL-1β, TNF-α, and others), which recruit circulating leukocytes (particularly, neutrophils and monocytes) to the site of inflammation.[8,9] The ECs also begin expressing elevated levels of cellular adhesion molecules (CAMs; these include ICAM-1, E-Selectin, VCAM-1, PECAM-1, and others) which facilitate, via receptor-ligand binding, leukocyte rolling and firm adhesion onto the endothelium – a necessary precursor to leukocyte transmigration into the tissue space to remove the source of inflammation.[10] Researchers have taken advantage of this overexpression of inflammation-associated CAMs for targeted therapy in several inflammatory diseases by designing particle drug carriers decorated with antibodies and ligands with binding specificity to these molecules.[11,12] To this end, several works have thoroughly investigated the impact of various particle parameters on the targeting efficacy of particulate drug carriers, including particle size[13–17], shape[13,18–21], and surface chemistry[22–25], resulting in a deep understanding of the interplay between these properties and ultimate drug carrier efficiency.

However, a major gap has emerged in prior works evaluating targeted drug carrier functionality. Specifically, it is well-established (and built into the conceptual design) that vascular-targeted drug carriers occupy the same physical space near the vascular wall and compete for the same binding sites as leukocytes in blood flow[4,20,26–29]. Additionally, it is well-understood that cellular collisions in blood flow are a major driver of hemodynamics[14,30,31]. Thus, the presence of vascular-targeted micro-or-nanoscale particles in the bloodstream is likely to impact leukocyte adhesion and response to inflammation. Further, neutrophils were recently reported to rapidly internalize particles in blood *in vivo* in mice, which prevents neutrophils from binding to the vascular wall, and it has been shown that the use of particle drug carriers can ameliorate the immune response in conditions such as West Nile Virus, EAE, and sepsis.[32–34] Indeed, prior studies have shown that biomimetic drug carriers are effective at both modulating the inflammatory immune response and delivering anti-inflammatory therapeutics to the site of inflammation, suggesting the potential for competition between drug carriers and leukocytes for binding sites on the vasculature.[35–39] Despite this, no work has systematically explored the impacts of leukocyte and drug carrier interactions (including cell-particle collision, competitive binding, and phagocytosis) on the functionality of these cells in human blood.

In this work, we demonstrate that both non-targeted and targeted model drug carriers inhibit leukocyte adhesion in human blood, dependent on particle concentration and size. Additionally, we find that internalization of particles leads to phenotypic changes in neutrophils (increasing CD11b expression and decreasing CD62L expression; importantly, CD11b binds to ICAM-1, which mediates firm adhesion, while CD62L is involved in the initial capture and slow rolling of neutrophils[9,40]) dependent on particle surface chemistry, which translate to faster leukocyte rolling velocity and reduced adhesion. Finally, we find that the magnitude of this effect varies with vessel size, likely due to changes in hemodynamics and cell-free layer (CFL) size in differently-sized vessels. These results have significant impacts for the design and efficacy of vascular-targeted drug carriers and shed new light on the previously-unexplored effects of vascular-targeted carriers on leukocytes.

Results

Targeted and non-targeted particles reduce white blood cell (WBC) adhesion in human blood flow

To investigate the impacts of the presence of particle drug carriers on WBC adhesion, we employed an *in vitro* parallel plate flow chamber (PPFC) assay as previously described.[14] For these experiments, human umbilical vein endothelial cells (HUVEC) were cultured on glass coverslips and activated for 4 hours with IL-1β prior to flow. Blood (with or without particles) was perfused over the monolayer in a pulsatile profile for 15 minutes as previously described.[14,15] For these experiments, sialyl Lewis A was chosen as a targeting ligand due to its high affinity for E-Selectin and ease of conjugation to our particle platform, and IgG was used as a non-targeted control to dampen non-specific interactions between particles and HUVEC.

When sialyl Lewis A-conjugated (“targeted”) polystyrene spheres were introduced, we visibly observed a drastic reduction in WBC adhesion. Exploring this effect in-depth,

we performed these experiments across a range of particle sizes (200 nm to 5 μm) and concentrations (5E5/mL through 1E9/mL; note: nanoparticles were tested at higher concentrations in order to achieve a "mass-based" dose on the same order of magnitude as the microparticles, and because little to no effect was seen for the nanoparticles at lower particle concentrations) and found some striking trends. First, we find minimal reduction in WBC adhesion for the 200 nm particles, even at high particle concentrations (Figure 1A). Moving forward, we see that the effect is concentration-dependent, with more significant inhibition of WBC adhesion generally occurring at higher particle concentrations. For example, focusing on the 500 nm spheres, we find that at a concentration of 5E5/mL, minimal reduction in WBC adhesion occurs (~10%); however, at a concentration of 1E9/mL, we find a much greater reduction in adhesion (~70%). (Figure 1B). This effect holds across all particle sizes tested except for 200 nm particles, suggesting that a greater number of leukocyte-particle collisions and greater endothelium surface coverage results in a more significant reduction in WBC adhesion.

Further, we find a major impact of particle size on reduction in leukocyte adhesion, with larger particles generally resulting in a more significant decrease in leukocyte adhesion, which is likely due to more-efficient margination to the CFL for larger particles[14,15]. For example, if we compare 500 nm (Figure 1B) and 2 μm particles (Figure 1C) at a concentration of 1E8/mL, we observe a reduction of ~20% in leukocyte adhesion for the 500 nm particles and ~100% for the 2 μm particles. Comparing 2 μm (Figure 1C) to 3 μm (Figure 1D) particles at a concentration of 1E7/mL, we find a percent reduction of ~70% for the 2 μm particles and a percent reduction of ~100% for the 3 μm particles. Similarly, if we compare 2 μm to 5 μm particles (Figure 1E) at a concentration of 1E7/mL, we find a percent reduction of ~70% for the 2 μm particles and a percent reduction of ~100% for the 5 μm particles.

Next, we sought to determine whether this effect was driven primarily by particle-leukocyte collisions or by specific blocking of binding sites on the endothelium by comparing the reduction in leukocyte adhesion for IgG-conjugated ("non-targeted") particles to targeted particles at the same size. For this comparison, we computed the 'Normalized Leukocyte Adhesion Ratio' using Equation 1 below:

$$Norm.\ Adhesion\ Ratio = \frac{\left(\frac{\#\ of\ adherent\ leukocytes\ for\ non-targeted\ particles}{\#\ of\ adherent\ leukocytes\ in\ particle\ free\ control}\right)}{\left(\frac{\#\ of\ adherent\ leukocytes\ for\ targeted\ particles}{\#\ of\ adherent\ leukocytes\ in\ particle\ free\ control}\right)} \quad (1)$$

Thus, a normalized leukocyte adhesion ratio (NAR) above 1 signifies a greater reduction in leukocyte adhesion for targeted particles versus non-targeted particles, with greater values signifying a greater effect. (Note: due to limitations in blood volume and cells, experiments were sometimes performed on different days and normalized to different controls, and thus the denominators in Equation 1 do not strictly cancel one another).

Figure 2A is a visual representation of the reduction in leukocyte adhesion for targeted particles versus non-targeted particles. Using the NAR analysis, we can determine

conditions at which particle targeting confers an additional reduction in leukocyte adhesion (Figure 2 B-F). A few findings stand out in this analysis. First, the added reduction in leukocyte adhesion for targeted particles primarily occurs with larger (micron-scale) particles, where the 2 μm, 3 μm, and 5 μm particles all exhibit NAR values much greater than 1 at higher particle concentrations (Figure 2 D-F). The greater impact of micron-sized particles on cell adhesion is likely due to larger particles localizing more efficiently to the vascular wall and, once bound, occupying more physical space and receptor binding sites on the endothelium. Nano-sized particles are less efficient at marginating[14,15]; thus, they likely reduce leukocyte adhesion primarily through physical interactions in free stream. Hence, we observe low NAR values for nanospheres (Figure 2 B, C). Indeed, we observe nanoparticles associating with leukocytes in blood flow, which supports this hypothesis (Supplemental Figure 1).

Additionally, we primarily see high NAR values at high particle concentrations, suggesting that the specific targeting impact on leukocyte adhesion occurs primarily when bound particles occupy a large portion of the endothelium. Indeed, when plotting particle adhesion versus percent reduction in leukocyte adhesion, we find that as particle adhesion increases, the percent reduction in leukocyte adhesion also increases, particularly for larger particles (Supplemental Figure 2). This trend of adhesion versus %reduction in leukocyte adhesion supports the notion that, once a certain fraction of the available space for binding on the endothelium is occupied, targeted particles out-compete circulating leukocytes and prevent them from binding. Further, when plotting % reduction in leukocyte adhesion versus HUVEC surface coverage percentage for targeted particles, we find the greatest reduction in leukocyte adhesion (and the greatest NAR values) once surface coverage reaches above ~10%. This observation suggests that perhaps at lower particle concentrations, nonspecific collisions are responsible for the observed reduction in leukocyte adhesion, but once a certain level of surface coverage is achieved via active targeting, the surface blocking effect begins to dominate (Supplemental Figure 3). Note: a direct comparison of percentage reduction in leukocyte adhesion for targeted versus untargeted particles is shown in Supplemental Figure 4; these data also illustrate the enhanced effect of collisions as both particle size and concentration increase, as well as the greater difference between targeted and non-targeted particles at higher particle concentrations. Additionally, some representative individual percent reduction data are shown in Supplemental Figure 5.

Inhibition of leukocyte adhesion in smaller blood vessels

Because hemodynamics can vary in blood vessels of varying sizes[41], we repeated a subset of the experiments from Figure 1 in a smaller channel (127 μm versus 254 μm channel height). These experiments are important for understanding if and how the observed reduction in leukocyte adhesion might manifest in blood vessels of varying sizes, informing the design of vascular-targeted drug carriers based on their intended destination. Thus, we evaluated leukocyte adhesion in the presence of 500 nm and 2 μm particles across a range of particle concentrations in the 127 μm channel. These results are presented in Figure 3.

First, we find that some of the same trends observed in the 254 μm channel emerge here. In general, a higher particle concentration results in a more significant reduction in leukocyte

adhesion. For example, the addition of non-targeted 500 nm spheres in blood at 1E7/mL results in a ~15% reduction in leukocyte adhesion, while a higher concentration of 1E9/mL leads to a 50% reduction in adhesion (Figure 3A). Similarly, for 2 μm non-targeted particles at 1E6/mL, we observe a ~30% reduction in leukocyte adhesion versus a ~60% reduction for 2 μm non-targeted particles at a concentration of 1E8/mL (Figure 3B). Because we again observe greater reduction in leukocyte adhesion for higher concentrations of both targeted and non-targeted particles, this suggests that both greater numbers of collisions and higher specific blocking of the endothelial surface result in decreased leukocyte adhesion in the 127 μm channel, similar to the 254 μm channel. Additionally, similar to the results in Figure 2, we see that larger particles generally result in a more significant reduction in leukocyte adhesion.

However, we do observe some changes in the smaller channel versus the larger channel. Notably, the overall magnitude of the percent reduction in leukocyte adhesion is generally lower in the smaller channel versus the larger channel, particularly for the 2 μm particles. This could be due to the changes in the relative size of the CFL and RBC core in the different vessels; theoretical and experimental results have shown that, as vessel size increases, the relative size of the cell-free layer decreases.[42] Thus, in a larger vessel, leukocytes and particle drug carriers will be pushed closer to the wall, likely resulting in more collisions, which in turn results in a greater inhibition in leukocyte adhesion. This hypothesis is also supported by experimental work from our lab showing that 2 μm particles marginate more efficiently in larger channels, while 500 nm particle margination is relatively unchanged.[14] However, calculations based on previous computational work show that, for a 127 μm channel versus a 254 μm channel, the CFL size will be approximately equivalent (3.25 μm versus 3.15 μm, respectively).[43] Thus, the differences observed could be simply due to a lower overall flow rate in the 127 μm channel, leading to a reduction in the magnitude of collision forces between particles and leukocytes. Of course, computational and many experimental works evaluate the CFL based on actual blood vessels, which may differ slightly from PPFC experiments.

Particle phagocytosis results in reduced leukocyte adhesion in blood flow *in vitro*

Given our recent work demonstrating that particle phagocytosis and clearance in mice *in vivo* results in a diversion of neutrophils to the liver[32], we sought to investigate whether particle internalization similarly influences adhesion for human leukocytes. Thus, we performed a series of experiments evaluating leukocyte adhesion in the presence of carboxylated and sialyl Lewis A-conjugated particles, where particles were either preincubated (1 hr) with cells prior to performing the flow experiments or introduced immediately prior to the flow experiment (i.e., the “Non-incubated” condition). Thus, for the “Preincubated” condition, particle phagocytosis was allowed to occur prior to blood flow, while for the “Non-incubated” condition, we expect particle phagocytosis to be minimal. The 1 hour incubation time was chosen for incubation time based on our previous work showing that appreciable particle phagocytosis occurs after approximately 1 hour in human blood *ex vivo*.[5] In addition, we used ACD for the non-phagocytic experiments because it chelates Ca^{2+}, preventing phagocytosis, and heparin was used for the preincubated condition as it anticoagulates by activating antithrombin III, which in turn deactivates Thrombin,

Factor IX, and Factor X, thus allowing for phagocytosis to occur. We performed these experiments with both 2 μm (at 1E7/mL) and 500 nm particles (at 6.4E8/mL; chosen for equivalent particle mass to the 2 μm particles); the results are shown in Figure 4.

Notably, we see a striking difference between the “Non-incubated” and “Preincubated” conditions for both particle sizes. For 2 μm particles in the “Non-incubated” condition, we see little to no reduction in leukocyte adhesion for the non-targeted particle and ~30% reduction for the sialyl Lewis A-targeted particles (Figure 4A). However, for the “Preincubated” condition, we find that both particle types significantly reduce leukocyte adhesion at close to the same level (~30% reduction for non-targeted, ~50% reduction for sLe^A). This observation for the 2 μm size is replicated with the 500 nm particles; for the “Non-incubated” condition, we find ~15% reduction for the non-targeted particles and ~50% reduction for the sLe^A particles, and for the “Preincubated” condition we find a reduction of ~75% for both particle types (Figure 4B).

These results have a few major implications. First, we find that particle internalization can dramatically reduce the propensity for leukocytes to adhere to an activated endothelium. Additionally, we see that the added component of internalization eliminates much or all of the difference between targeted and non-targeted particles, suggesting that phagocytosis dominates in this effect over particle-leukocyte collisions and specific blocking of binding sites on the endothelium. This finding is critically important, as it more closely describes the situation found *in vivo*.

Particle phagocytosis results in altered neutrophil phenotype, changing ligand expression levels

The results in Figure 4 led us to ask whether particle phagocytosis results in specific changes in the leukocyte phenotype, which drive the reduction in leukocyte adhesion further. Because neutrophils comprise up to 70%[44] of circulating leukocytes and are the primary first-responders in inflammation, monocytes are responsible for relatively little particle uptake in *ex vivo* blood samples (~20% particle positive monocytes, Supplemental Figure 6), and given recent work showing that neutrophil-particle interactions impact the immune response to inflammation *in vivo*[32,45], we focus this analysis on neutrophils. Further, we performed flow cytometry on whole blood samples from 3 blood donors showing that, before PPFC experiments, ~62% of leukocytes are neutrophils, while after perfusion in the PPFC ~50% of leukocytes in the outlet are neutrophils, suggesting that neutrophils are overrepresented in the adherent cell population (Supplemental Figure 7). Additionally, given our recent work showing that particle surface chemistry greatly impacts neutrophil phagocytosis[5], (specifically, PEGylation results in greater uptake by human neutrophils in blood and plasma), we investigated these changes resulting from phagocytosis of carboxylated polystyrene particles, PEGylated polystyrene particles, and sialyl Lewis A-conjugated particles (Figure 5). For these experiments, we incubated heparinized human whole blood with 2 μm particles of the various surface chemistries for 2 hours, allowing for phagocytosis to occur. Then, we stained the samples for CD11b and CD62L and measured their expression levels via flow cytometry, comparing the expression levels to untreated samples. Notably, we found that neutrophils exposed to all particle types increased their

expression of CD11b, by a factor of ~2 for PS-COOH and PS-sLe^A particles and by a factor of ~2.5 for PS-PEG particles (Figure 5A). Further, we found that this effect is more pronounced in particle-positive neutrophils, with fold increases of CD11b expression of ~2.5 for PS-COOH and PS-sLe^A and ~3 for PS-PEG (Figure 5B). As expected with an increase in CD11b expression, we find that particle internalization results in a reduction in CD62L expression by a factor of ~1.5 for PS-COOH and PS-sLe^A and ~2 for PS-PEG, with similar reductions in expression for particle-positive neutrophils (Figure 5 C-D). These results show that, in general, particle uptake significantly alters neutrophil phenotype, which can result in downstream effects on neutrophil (and, thus, leukocyte) functions. Further, we see that, because neutrophils more-readily phagocytose PS-PEG particles, this induces a greater change in CD11b and CD62L expression, resulting in weaker adhesion kinetics and thus faster neutrophil rolling on the endothelial surface (Supplemental Figure 8).

Discussion

While targeted drug carriers have been widely researched over the past several decades for their potential to protect therapeutic molecules from degradation and deliver drug directly to the site of disease, there is still much we do not understand about their potential side effects, especially in humans. Additionally, very few of these formulations have successfully passed clinical trials, suggesting a need for more rigorous studies of the potential side effects of injectable particle drug carrier platforms. In this work, we aimed to investigate the impact of model drug carriers on the behavior and function of leukocytes broadly and neutrophils specifically in blood flow, as these impacts have not been thoroughly explored previously.

Importantly, we found that the introduction of both targeted and non-targeted polymeric particles results in significantly reduced leukocyte adhesion to an inflamed endothelium *in vitro* (Figures 1–3). This effect was highly dependent on both particle size and particle concentration, with larger particles and higher particle concentrations generally resulting in greater inhibition in leukocyte adhesion. Thus, it is possible that certain particle formulations/dosing schemes may result in a more pronounced impact, informing the design parameters for such formulations. Additionally, we find that, for certain particle sizes and concentrations, there is a significant increase in the reduction of leukocyte adhesion when particles are targeted to the site of inflammation (Figure 2), suggesting that both physical collisions and specific competition for binding sites on the endothelium are at play in this effect. Again, this finding reinforces the need to consider whether reducing leukocyte adhesion at the site of inflammation will result in unintended side effects.

Additionally, we found that vessel size is another important factor in the prominence of this effect. Because blood vessel size impacts the size of the CFL and particle margination efficacy[14,42], as well as the magnitude of collision forces in blood flow, it also affects how frequently particles and leukocytes will collide. Thus, we observe that the reduction in leukocyte adhesion is somewhat less prominent in a smaller chamber, particularly for the 2 μm particles, which carries important implications depending on the desired destination of a given particle drug carrier (Figure 3).

Given that neutrophils are by far the most abundant blood leukocyte, comprising up to 70% of all circulating white blood cells[44], as well as recent work in our lab and others showing that neutrophil-particle interactions *in vivo* drive changes in the immune response to inflammation[32,45], we focused the remainder of our analysis on neutrophils specifically. Despite their relative prevalence, very little of the literature examining the internalization of particle drug carriers has examined the phagocytic contributions of neutrophils, leading to a gap in understanding that is only recently being filled. Indeed, recent work by Kelley et al. shows that neutrophils phagocytose particle drug carriers very different from cultured or isolated macrophages and monocytes which are frequently used for phagocytosis studies.[5] Notably, monocytes, the other major population of circulating phagocytes, exhibit very little particle phagocytosis *ex vivo* (Supplemental Figure 6). Thus, when evaluating the effects of phagocytosis on leukocyte adhesion, it makes sense to specifically hone in on neutrophils.

In these studies, we found that, in addition to particle-leukocyte collisions, particle phagocytosis is another major driver of altered leukocyte behavior in human blood (Figures 4–5, Supplemental Figure 8), which is in agreement with our recent work in mice.[32] Based on previous work, and because the polystyrene spheres are not specifically targeted to any ligands on the neutrophil surface, we expect that the particle will rapidly undergo opsonization with plasma proteins, which facilitates interaction with the with FC receptors on the neutrophil surface. The engagement of Fc receptors is known to initiate cell eating.[46,47] We observe that particle internalization results in increased expression of CD11b and shedding of CD62L for neutrophils, and that this effect varies depending on the particle surface chemistry (Figure 5). These results are consistent with neutrophil activation. Further, we see that these changes are correlated with downstream changes in neutrophil function, resulting in decreased firm adhesion (Figure 4) and increased rolling velocity and proportion of rolling neutrophils versus firmly adherent (Supplemental Figure 8). These results, upon first glance, may seem counterintuitive as reduced CD62L expression and increased CD11b expression are typical of neutrophil activation.[9] However, in the context of the normal inflammation and cell adhesion cascade, neutrophil activation occurs after the initial capture to the endothelium and rolling adhesion step. As L-selectin is a critical molecule for the initial capture, the pre-activation of these cells in circulation via particle internalization will lead to reduced adhesion.[9]

Importantly, we find that particle phagocytosis eliminates significant differences between the impact of targeted and non-targeted particles on leukocyte adhesion, implying that phagocytosis is the dominating driver of this effect. Thus, if a drug carrier is modified with a coating that greatly reduces phagocytosis by circulating leukocytes, it is possible that this effect (or at least the phagocytosis-driven portion of it) will be sufficiently muted. However, the typical approach for achieving a non-fouling drug carrier surface, i.e., PEGylation, was recently reported to promote phagocytosis in human neutrophils, suggesting other approaches are needed.[5] Here, the use of zwitterionic coatings[48–50] or leukocyte mimetic surfaces[35,36] may be the key to reducing phagocytosis of particle drug carriers by circulating leukocytes in human blood and avoiding the reduction in leukocyte adhesion observed in this work.

Additionally, other strategies may be employed to alter particle margination, the magnitude of collision forces, particle phagocytosis, or some combination of these. It has been reported that changing particle shape can alter both particle margination dynamics[20] and phagocytosis[19,51], both of which would likely alter the magnitude of the reduction in leukocyte adhesion observed here. Further, manipulating the stiffness of particles can impact margination dynamics, collision forces, and particle phagocytosis[52–54], with softer particles resulting in lower collision forces and potentially decreased phagocytosis by circulating leukocytes. Thus, a thorough exploration of how these particle properties influence the reduction in leukocyte adhesion observed here could reveal strategies for mitigating this effect on the efficacy of drug delivery systems.

The results presented in this study have a wide range of implications for the field of particle drug delivery across a wide range of applications. First and foremost, the surface blocking mechanism of leukocyte adhesion reduction only applies to applications where particle drug carriers are targeted to inflammatory molecules (or potentially other surface molecules) on the vascular wall, and may not be a concern for passive targeting schemes or otherwise non-targeted particles. Second, these effects may be undesirable in certain contexts (e.g., by preventing leukocytes from adhering/transmigrating to destroy a pathogen), but desirable in others (e.g., preventing an overactive immune response such as those seen in certain autoimmune diseases which result in downstream thrombus formation). Of course, the non-specific collision and phagocytosis mechanisms apply to all contexts, and again could be beneficial or not depending on the disease context. For example, one of the most prominent and widely-studied applications for targeted drug delivery is for the delivery of cancer therapeutics. Given the immunosuppressive tumor microenvironment is a major obstacles to cancer treatment, i.e., immune cells fail to recognize and destroy cancer cells, the effects observed in these studies may result in decreased efficacy for particle drug carriers for cancer therapy.[55] On the other hand, tumor-associated neutrophils have recently emerged as a potential therapeutic target as neutrophils have been shown to promote tumorigenesis and metastasis.[56] Thus, the exact impact of these effects on drug carriers for cancer therapies is at question, and should be evaluated by groups involved in designing drug carriers for cancer applications.

It is important to highlight a few limitations to work presented in this manuscript. First, all of the experiments described in this study utilized polystyrene spheres as model particulate drug carriers. While these are an excellent and convenient model for evaluating drug carrier properties, they do not necessarily always directly predict the behavior of actual drug carriers made from biocompatible materials, particularly because the efficiency and effect of neutrophil phagocytosis can vary greatly based on particle material.[57] Thus, employing particle drug carriers comprised of such materials (such as PLGA), may not result in the same effects seen here. Furthermore, while this study focuses specifically on the impact of leukocyte-particle interactions on neutrophil adhesion, we recognize that neutrophils also exercise other important functions in inflammation, including oxidative burst, degranulation, and NETosis. Thus, future work focusing on these other aspects of neutrophil behavior in inflammation may be necessary to shed more light on the totality of the impact of particle drug carriers on neutrophil function in inflammation. In particular, NETosis is an interesting phenomenon which often contributes to the damage caused by neutrophils

in inflammatory diseases.[40,58] Typically, NETs are released after neutrophils transmigrate through the endothelium to destroy the cause of inflammation.[59,60] Thus, we expect that the prevention of neutrophil adhesion would reduce NETosis at the site of acute inflammation. However, there is evidence that in some chronic inflammatory conditions, e.g., autoimmune conditions, neutrophils are 'preactivated' and may release NETs into circulation.[61–63] Thus, further exploration into the impact on intravenously-administered particle drug carriers on activated neutrophils and NETosis in circulation is warranted, though outside the scope of this paper.

Conclusions

Overall, this work demonstrates for the first time that polymeric drug carriers may have unintended effects on the ability of leukocytes to respond to an inflammatory event. Because drug carriers and leukocytes will necessarily be occupying the same physical space near and on the vascular wall, particularly in the case of vascular-targeted carriers which are designed to bind to inflammatory molecules, leukocytes and drug carriers (especially neutrophils) will interact with one another intimately in blood flow, potentially hindering the ability of leukocytes to bind to the endothelium. This could have unintended consequences for patients being treated with a drug carrier formulation, and might contribute to the general failure of drug carrier formulations advancing past clinical trials and onto the market. Additionally, we find that particle uptake dramatically inhibits the ability of human neutrophils to bind to an inflamed endothelium, in concurrence with our previous work[32]. However, that result suggests that this effect can perhaps be mitigated by sufficiently protecting drug carriers from phagocytosis, which is beneficial for drug carrier efficacy already. Additionally, these results suggest that there may be opportunities to effectively target circulating leukocytes simply by designing particles which will accumulate near the vascular wall, perhaps enhancing any such therapeutic strategy. In the grand scheme, this study provides crucial information as to how drug carriers interact with leukocytes in blood flow, and will help inform the design of particle drug carriers in the future.

Methods

Study Approvals

Human blood was obtained from healthy donors via venipuncture per a protocol approved by the University of Michigan Internal Review Board. Informed, written consent was obtained from donors prior to blood collection.

Particle Functionalization

Fluorescent, carboxylated polystyrene (5 μm, 3 μm, 2 μm, and 500 nm, Polysciences, Inc.) were conjugated with IgG or sialyl Lewis A via avidin proteins covalently linked to the particle surface using carbodiimide chemistry.[64] Briefly, carboxylated particles were washed with 50 mM 2-(N-morpholino)ethanesulfonic acid (MES) buffer, then resuspended in a 5 mg/mL NeutrAvidin® solution and rotated at room temperature for 15 minutes, at which time an equivalent volume of 75 mg/mL *N*-(3-Dimethylaminopropyl)-*N*′-ethylcarbodiimide hydrochloride (EDC, Sigma) was added, and particles were rotated overnight. After

overnight incubation, 7.5 mg/mL of glycine (Sigma) was added to the solution, and particles were rotated for another 15 minutes. Then, particles were washed with 50 mM PBS buffer, counted via fluorescence microscopy using a hemacytometer, and stored at 4° C.

After NeutrAvidin® conjugation, particles were then conjugated with either biotinylated rat IgG2b (Biolegend) or sialyl Lewis A (Glycotech). This was achieved by a 45-minute incubation with the desired ligand on a rotator, after which particles were stored in a PBS buffer with calcium and magnesium ions and 1% BSA until use or site density characterization. Site densities were determined via flow cytometry using anticutaneous-lymphocite-associated-antigen-APC (for sLeA; Miltenyi Biotech) or anti-rat-IgG2b-PE (for IgG, eBioscience) as previously described.[65] Site densities for both sLeA and IgG were fixed at ~2000 sites/μm^2, consistent with previous experiments.

For PEGylated particles, NeutrAvidin® was substituted for 30 mg/mL of aminated, methoxy-terminated polyethylene glycol (PEG, 5k molecular weight, Fisher), as described previously.[5]

Cell Culture and HUVEC Monolayer Preparation

Human umbilical vein endothelial cells (HUVEC) were isolated from umbilical cords obtained from Mott Children's Hospital at the University of Michigan. Isolated HUVEC were cultured in T75 flasks at 37°C and 5% CO_2 until confluent, and then seeded onto glass coverslips coated with gelatin as previously described.[66] Monolayers were allowed to grow to confluence prior to use, typically over the course of 48 hours.

Parallel plate flow chamber assays

Venous blood was collected from healthy adults into a syringe using either acid-sodium citrate-dextrose (ACD, for non-phagocytic experiments) or heparin-sodium (for phagocytic experiments) as anticoagulant. Confluent HUVEC monolayers were activated with 2 mL of 10ng/mL IL-1β (Fitzgerald) for 4 hours prior to flow experiments to induce CAM expression. After activation, blood with or without particles was perfused over the activated HUVEC monolayer using a parallel pate flow chamber (PPFC, Glycotech) and syringe pump.

For pulsatile flow experiments (Figures 1, 3, and 5), blood was perfused forward for 14 seconds and backward for 7 seconds at a shear rate of $1000s^{-1}$, for a total of 15 minutes. The $1000s^{-1}$ shear rate and pulsatile flow profile were chosen to simulate the shear rate of arterial blood flow[67,68] and conditions relevant in vessels often associated with coronary artery disease, one condition where targeted particle drug carriers would be employed.[14,69] For laminar flow experiments (Figure 4), blood was perfused forward over the monolayer for a total of 5 minutes at a shear rate of $1000s^{-1}$. A 5-minute time was chosen for laminar flow experiments in order to establish a fully-developed laminar flow profile, while 15 minutes was chosen for pulsatile experiments to match the blood volume used in laminar flow experiments. For both types of experiments, after perfusion was completed, PBS with calcium and magnesium ions and 1% BSA was added and perfused at a shear rate of $500s^{-1}$ while images or videos were taken. For leukocyte counts, 10 images were taken

along the length of the flow chamber using a Nikon TE-2000-S microscope with a digital camera (Photometrics CoolSNAP EZ with a Sony CCD sensor), and cells were counted using ImageJ software. For rolling velocity analysis, 10-second videos were taken for each sample, and rolling leukocytes were tracked using NIS-Elements® software.

Blood flow rates were determined based on the shear rate and channel size using Equation 2, below:

$$\gamma = \frac{6Q}{h^2 w} \tag{2}$$

where γ (s^{-1}) is the shear rate, Q is the volumetric flow rate (mL/s), h is the channel height (0.127 or 0.254 cm), and w is the channel width (0.25 cm).

For phagocytic flow experiments, particles at the desired concentration were added to blood 1 hour prior to flow, allowing for a substantial amount of particle uptake as previously characterized.[5]

Particle uptake and neutrophil phenotype assays

Particle uptake assays were performed as previously described.[5] Briefly, venous blood was collected from healthy adults into a syringe using heparin-sodium as an anticoagulant. 100 μL aliquots were distributed into FACS tubes, and 5 μL of particle solution in PBS was added for a final concentration of 1E7/mL for 2 μm particles and 6.4E8/mL for 500 nm particles. Samples were incubated at 37°C and 5% CO_2 for 1 hour, and were then stained using CD45-APC, CD11b APC-Cy7, and CD62L PE-Cy7 (Biolegend) on ice for 30 minutes. 2 mL of 1-step Fix-Lyse solution (eBiosciences) was then added to each sample, and the samples were allowed to sit at room-temperature for 30 minutes. Fixed samples were then washed 3x with FACS buffer (PBS −/− w/ 2% fetal bovine serum (FBS), pH 7.4) and analyzed using flow cytometry.

Untreated samples were used as a control for normalization of expression levels and for gating ‘particle positive’ cells. Neutrophils were gated as previously described.[5] Expression levels are reported as fold changes over the untreated samples, with reductions being reported as the negative reciprocal of the decimal for proper visual scaling.

Neutrophil isolation

For experiments with isolated neutrophils (Figure 4), neutrophils were isolated from whole blood and then reconstituted as follows. Venous blood was collected from healthy adults into syringes using heparin-sodium as an anticoagulant. 20 mL of blood was then layered on top of 20 mL of lymphoprep (Fresenius Kabi Norge AS). The top plasma layer was then collected using a pasteur pipette and stored at room temperature. The middle layer, containing monocytes and lymphocytes, was discarded along with the lymphoprep layer. The RBC/neutrophil pellet was preserved, and plasma was added back to the solution. Then, PBS containing calcium and magnesium ions with 1% BSA was added to return the final volume to 20 mL to preserve a physiological concentration of neutrophils.

Neutrophils were then allowed to phagocytose particles as described above and used for flow experiments.

Statistical Methods

Data from flow experiments is representative of trials using at least 3 independent donors. Uptake studies are representative of trials using at least 3 independent donors, with duplicates for each. For all studies, all data points were included in the analysis. Data are plotted with standard error. Significance was determined by ANOVA using GraphPad Prism. Asterisks indicate p values of: * = $p < 0.05$, ** = $p < 0.01$, *** = $p < 0.001$. n.s. indicates "not significant".

Supplementary Material

Refer to Web version on PubMed Central for supplementary material.

Acknowledgments

This work was supported by the National Science Foundation Graduate Research Fellowship Program (W.J.K.), the University of Michigan's Postdoctoral Fellowship (C.A.F), and NIH R01 HL115138 (O.E.A.).

References

(1). Bennet D; Kim S. Polymer Nanoparticles for Smart Drug Delivery. In Application of Nanotechnology in Drug Delivery; 2014; pp 257–310. 10.5772/58422.

(2). Singh RW,LJ;Nanoparticle-Based Targeted Drug Delivery. Exp. Mol. Pathol. 2009, 86 (3), 215–223. 10.1016/j.yexmp.2008.12.004.Nanoparticle-based. [PubMed: 19186176]

(3). Couvreur P. Nanoparticles in Drug Delivery: Past, Present and Future. Adv. Drug Deliv. Rev. 2013, 65 (1), 21–23. 10.1016/j.addr.2012.04.010. [PubMed: 22580334]

(4). Namdee K; Thompson AJ; Charoenphol P; Eniola-Adefeso O. Margination Propensity of Vascular-Targeted Spheres from Blood Flow in a Microfluidic Model of Human Microvessels. Langmuir 2013, 29 (8), 2530–2535. 10.1021/la304746p. [PubMed: 23363293]

(5). Kelley WJ; Fromen CA; Lopez-Cazares G; Eniola-Adefeso O. PEGylation of Model Drug Carriers Enhances Phagocytosis by Primary Human Neutrophils. Acta Biomater. 2018, 79, 283–293. 10.1016/j.actbio.2018.09.001. [PubMed: 30195083]

(6). Anselmo AC; Mitragotri S. Nanoparticles in the Clinic. Bioeng. Transl. Med. 2016, 1 (1), 10–29. 10.1002/btm2.10003. [PubMed: 29313004]

(7). Fujiwara Y; Mukai H; Saeki T; Ro J; Lin YC; Nagai SE; Lee KS; Watanabe J; Ohtani S; Kim SB; et al. A Multi-National, Randomised, Open-Label, Parallel, Phase III Non-Inferiority Study Comparing NK105 and Paclitaxel in Metastatic or Recurrent Breast Cancer Patients. Br. J. Cancer 2019, 120 (5), 475–480. 10.1038/s41416-019-0391-z. [PubMed: 30745582]

(8). Chen L; Deng H; Cui H; Fang J; Zuo Z; Deng J; Li Y; Wang X; Zhao L. Inflammatory Responses and Inflammation-Associated Diseases in Organs. Oncotarget 2018, 9 (6), 7204–7218. [PubMed: 29467962]

(9). Sadik CD; Kim ND; Luster AD Neutrophils Cascading Their Way to Inflammation. Trends Immunol. 2011, 32 (10), 452–460. 10.1016/j.it.2011.06.008. [PubMed: 21839682]

(10). Golias CH; Tsoutsi E; Matziridis A; Makridis P; Batistatou A; Charalabopoulos K. Leukocyte and Endothelial Cell Adhesion Molecules in Inflammation Focusing on Inflammatory Heart Disease. In Vivo (Brooklyn). 2007, 21 (5), 757–770. https://doi.org/N/A.

(11). Decuzzi P; Ferrari M. Design Maps for Nanoparticles Targeting the Diseased Microvasculature. Biomaterials 2008, 29 (3), 377–384. 10.1016/j.biomaterials.2007.09.025. [PubMed: 17936897]

(12). Howard M; Zern BJ; Anselmo AC; Shuvaev VV; Mitragotri S; Muzykantov V. Vascular Targeting of Nanocarriers: Perplexing Aspects of the Seemingly Straightforward Paradigm. ACS Nano 2014, 8 (5), 4100–4132. 10.1021/nn500136z. [PubMed: 24787360]

(13). Decuzzi P; Godin B; Tanaka T; Lee SY; Chiappini C; Liu X; Ferrari M. Size and Shape Effects in the Biodistribution of Intravascularly Injected Particles. J. Control. Release 2010, 141 (3), 320–327. 10.1016/j.jconrel.2009.10.014. [PubMed: 19874859]

(14). Charoenphol P; Huang RB; Eniola-Adefeso O. Potential Role of Size and Hemodynamics in the Efficacy of Vascular-Targeted Spherical Drug Carriers. Biomaterials 2010, 31 (6), 1392–1402. 10.1016/j.biomaterials.2009.11.007. [PubMed: 19954839]

(15). Charoenphol P; Mocherla S; Bouis D; Namdee K; Pinsky DJ; Eniola-Adefeso O. Targeting Therapeutics to the Vascular Wall in Atherosclerosis-Carrier Size Matters. Atherosclerosis 2011, 217 (2), 364–370. 10.1016/j.atherosclerosis.2011.04.016. [PubMed: 21601207]

(16). Tilles a W.; Eckstein EC The Near-Wall Excess of Platelet-Sized Particles in Blood Flow: Its Dependence on Hematocrit and Wall Shear Rate. Microvasc. Res. 1987, 33 (2), 211–223. 10.1016/0026-2862(87)90018-5. [PubMed: 3587076]

(17). Champion J; Walker A; Mitragotri S. Role of Particle Size in Phagocytosis of Polymeric Microspheres. Pharm. Res. 2008, 25 (8), 1815–1821. 10.1007/s11095-008-9562-y.Role. [PubMed: 18373181]

(18). Geng Y.a N.; Dalhaimer P; Cai S; Tsai R; Minko T; Discher DE Shape Effects of Filaments versus Spherical Particles in Flow and Drug Delivery. Nat. Nanotechnol. 2007, 2 (4), 249–255. 10.1038/nnano.2007.70.Shape. [PubMed: 18654271]

(19). Champion JA; Mitragotri S. Shape Induced Inhibition of Phagocytosis of Polymer Particles. Pharm. Res. 2009, 26 (1), 244–249. 10.1007/s11095-008-9626-z. [PubMed: 18548338]

(20). Thompson AJ; Mastria EM; Eniola-Adefeso O. The Margination Propensity of Ellipsoidal Micro/Nanoparticles to the Endothelium in Human Blood Flow. Biomaterials 2013, 34 (23), 5863–5871. 10.1016/j.biomaterials.2013.04.011. [PubMed: 23642534]

(21). Roberts RA; Eitas TK; Byrne JD; Johnson BM; Short PJ; McKinnon KP; Reisdorf S; Luft JC; DeSimone JM; Ting JP Towards Programming Immune Tolerance through Geometric Manipulation of Phosphatidylserine. Biomaterials 2015, 72, 1–10. 10.1016/j.biomaterials.2015.08.040. [PubMed: 26325217]

(22). Vittaz M; Bazile D; Spenlehauer G; Verrecchia T; Veillard M; Puisieux F; Labarre D. Effect of PEO Surface Density on Long- Circulating PLA-PEO Nanoparticles Which Are Very Low Complement Activators. Biomaterials 1996, 17 (16), 1575–1581. [PubMed: 8842361]

(23). Walkey CD; Olsen JB; Guo H; Emili A; Chan WCW Nanoparticle Size and Surface Chemistry Determine Serum Protein Adsorption and Macrophage Uptake. J. Am. Chem. Soc. 2012, 134 (4), 2139–2147. 10.1021/ja2084338. [PubMed: 22191645]

(24). He C; Hu Y; Yin L; Tang C; Yin C. Effects of Particle Size and Surface Charge on Cellular Uptake and Biodistribution of Polymeric Nanoparticles. Biomaterials 2010, 31 (13), 3657–3666. 10.1016/j.biomaterials.2010.01.065. [PubMed: 20138662]

(25). Gref R; Lu M; Sud P; Pharmaceutiques E. ‘ Stealth ‘ Corona-Core Nanoparticles Surface Modified by Polyethylene Glycol (PEG): Influences of the Corona (PEG Chain Length and Surface Density) and of the Core Composition on Phagocytic Uptake and Plasma Protein Adsorption. Colloids Surfaces B Biointerfaces 2000, 18, 301–313. [PubMed: 10915952]

(26). Müller K; Fedosov D.a; Gompper G. Margination of Micro- and Nano-Particles in Blood Flow and Its Effect on Drug Delivery. Sci. Rep. 2014, 4 (4871). 10.1038/srep04871.

(27). Kumar A; Graham MD Mechanism of Margination in Confined Flows of Blood and Other Multicomponent Suspensions. Phys. Rev. Lett. 2012, 109 (10), 1–5. 10.1103/PhysRevLett.109.108102.

(28). Müller K; Fedosov DA; Gompper G. Understanding Particle Margination in Blood Flow – A Step toward Optimized Drug Delivery Systems. Med. Eng. Phys. 2015, 1–9. 10.1016/j.medengphy.2015.08.009.

(29). Goldsmith HL; Spain S. Margination of Leukocytes in Blood-Flow through Small Tubes. Microvasc Res 1984, 27 (2), 204–222. 10.1016/0026-2862(84)90054-2. [PubMed: 6708830]

(30). Gutierrez M; Fish MB; Golinski AW; Eniola-Adefeso O. Presence of Rigid Red Blood Cells in Blood Flow Interferes with the Vascular Wall Adhesion of Leukocytes. Langmuir 2018, 34 (6), 2363–2372. 10.1021/acs.langmuir.7b03890. [PubMed: 29347819]

(31). Huang RB; Mocherla S; Heslinga MJ; Charoenphol P; Eniola-Adefeso O. Dynamic and Cellular Interactions of Nanoparticles in Vascular-Targeted Drug Delivery. Mol. Membr. Biol. 2010, 27 (7), 312–327. 10.3109/09687688.2010.522117. [PubMed: 21028938]

(32). Fromen CA; Kelley WJ; Fish MB; Adili R; Hoenerho MJ; Holinstat M; Eniola-adefeso O. Neutrophil − Particle Interactions in Blood Circulation Drive Particle Clearance and Alter Neutrophil Responses in Acute In Fl Ammation. ACS Nano 2017, 11, 10797–10807. 10.1021/acsnano.7b03190.

(33). Saito E; Kuo R; Pearson RM; Gohel N; Cheung B; King NJC; Miller SD; Shea LD Designing Drug-Free Biodegradable Nanoparticles to Modulate Inflammatory Monocytes and Neutrophils for Ameliorating Inflammation. J. Control. Release 2019, 300 (December 2018), 185–196. 10.1016/j.jconrel.2019.02.025.

(34). Casey LM; Kakade S; Decker JT; Rose JA; Deans K; Shea LD; Pearson RM Cargo-Less Nanoparticles Program Innate Immune Cell Responses to Toll-like Receptor Activation. Biomaterials 2019, 218 (March), 119333. 10.1016/j.biomaterials.2019.119333.

(35). Parodi A; Quattrocchi N; Ven AL van de; Chiappini C; Evangelopoulos M; Martinez JO; Brown BS; Khaled SZ; Yazdi IK; Enzo MV; et al. Biomimetic Functionalization with Leukocyte Membranes Imparts Cell like Functions to Synthetic Particles. Nat. Nano 2013, 8 (1), 61–68. 10.1038/nature13314.A.

(36). Palomba R; Parodi A; Evangelopoulos M; Acciardo S; Corbo C; De Rosa E; Yazdi IK; Scaria S; Molinaro R; Furman NET; et al. Biomimetic Carriers Mimicking Leukocyte Plasma Membrane to Increase Tumor Vasculature Permeability. Sci. Rep. 2016, 6 (December 2015), 1–11. 10.1038/srep34422. [PubMed: 28442746]

(37). Corbo C; Cromer WE; Molinaro R; Toledano Furman NE; Hartman KA; De Rosa E; Boada C; Wang X; Zawieja DC; Agostini M; et al. Engineered Biomimetic Nanovesicles Show Intrinsic Anti-Inflammatory Properties for the Treatment of Inflammatory Bowel Diseases. Nanoscale 2017, 9 (38), 14581–14591. 10.1039/c7nr04734g.

(38). Molinaro R; Corbo C; Martinez JO; Taraballi F; Evangelopoulos M; Minardi S; Yazdi IK; Zhao P; De Rosa E; Sherman MB; et al. Biomimetic Proteolipid Vesicles for Targeting Inflamed Tissues. Nat. Mater. 2016, 15 (9), 1037–1046. 10.1038/nmat4644. [PubMed: 27213956]

(39). Martinez JO; Molinaro R; Hartman KA; Boada C; Sukhovershin R; De Rosa E; Kirui D; Zhang S; Evangelopoulos M; Carter AM; et al. Biomimetic Nanoparticles with Enhanced Affinity towards Activated Endothelium as Versatile Tools for Theranostic Drug Delivery. Theranostics 2018, 8 (4), 1131–1145. 10.7150/thno.22078. [PubMed: 29464004]

(40). Y K. Neutrophil Biology: An Update. EXCLI J. 2015, 14, 220–227. 10.17179/excli2015-102. [PubMed: 26600743]

(41). Kim S; Ong PK; Yalcin O; Intaglietta M; Johnson PC The Cell-Free Layer in Microvascular Blood Flow. Biorheology 2009, 46 (3), 181–189. 10.3233/BIR-2009-0530. [PubMed: 19581726]

(42). Bagchi P. Mesoscale Simulation of Blood Flow in Small Vessels. Biophys. J. 2007, 92 (6), 1858–1877. 10.1529/biophysj.106.095042. [PubMed: 17208982]

(43). Sharan M; Popel AS A Two-Phase Model for Flow of Blood in Narrow Tubes with Increased Effective Viscosity near the Wall. Biorheology 2001, 38 (5–6), 415–428. [PubMed: 12016324]

(44). Rosales C. Neutrophil : A Cell with Many Roles in Inflammation or Several Cell Types ? Front. Physiol. 2018, 9 (February), 1–17. 10.3389/fphys.2018.00113. [PubMed: 29377031]

(45). Saito E; Kuo R; Pearson RM; Gohel N; Cheung B; King NJC; Miller SD; Shea LD Designing Drug-Free Biodegradable Nanoparticles to Modulate Inflammatory Monocytes and Neutrophils for Ameliorating Inflammation. J. Control. Release 2019, 300 (February), 185–196. 10.1016/j.jconrel.2019.02.025. [PubMed: 30822435]

(46). Dale DC; Boxer L; Conrad Liles W. The Phagocytes: Neutrophils and Monocytes. Blood 2008, 112 (4), 935–945. 10.1182/blood-2007-12-077917. [PubMed: 18684880]

(47). Rosales C; Uribe-Querol E. Phagocytosis: A Fundamental Process in Immunity. Biomed Res. Int. 2017. 10.1155/2017/9042851.

(48). García KP; Zarschler K; Barbaro L; Barreto JA; Malley WO; Spiccia L; Stephan H; Graham B. Zwitterionic-Coated " Stealth " Nanoparticles for Biomedical Applications : Recent Advances in Countering Biomolecular Corona Formation and Uptake by the Mononuclear Phagocyte System. Small 2014, 10 (13), 2516–2529. 10.1002/smll.201303540. [PubMed: 24687857]

(49). Xiao W; Lin J; Li M; Ma Y; Chen Y; Zhang C; Li D; Gu H. Prolonged in Vivo Circulation Time by Zwitterionic Modification of Magnetite Nanoparticles for Blood Pool Contrast Agents. Contrast Media Mol. Imaging 2012, 7 (3), 320–327. 10.1002/cmmi.501. [PubMed: 22539402]

(50). Breus VV; Heyes CD; Tron K; Nienhaus GU Zwitterionic Biocompatible Quantum Dots for Wide PH Stability and Weak Nonspecific Binding to Cells. ACS Nano 2009, 3 (9), 2573–2580. 10.1021/nn900600w. [PubMed: 19719085]

(51). Champion J. a; Mitragotri, S. Role of Target Geometry in Phagocytosis. Proc. Natl. Acad. Sci. U. S. A. 2006, 103 (13), 4930–4934. 10.1073/pnas.0600997103. [PubMed: 16549762]

(52). Su J; Sun H; Meng Q; Yin Q; Tang S; Zhang P. Long Circulation Red-Blood-Cell-Mimetic Nanoparticles with Peptide-Enhanced Tumor Penetration for Simultaneously Inhibiting Growth and Lung Metastasis of Breast Cancer. Adv. Funct. Mater. 2016, 26, 1243–1252. 10.1002/adfm.201504780.

(53). Fish MB; Fromen CA; Lopez-Cazares G; Golinski AW; Scott TF; Adili R; Holinstat M; Eniola-Adefeso O. Exploring Deformable Particles in Vascular-Targeted Drug Delivery: Softer Is Only Sometimes Better. Biomaterials 2017, 124, 169–179. 10.1016/j.biomaterials.2017.02.002. [PubMed: 28209527]

(54). Anselmo AC; Zhang M; Kumar S; Vogus DR; Menegatti S; Helgeson ME; Mitragotri S. Elasticity of Nanoparticles Infl Uences Their Blood Circulation, Phagocytosis, Endocytosis, and Targeting. ACS Nano 2015, 9 (3), 3169–3177. [PubMed: 25715979]

(55). Liu Y; Zeng G. Cancer and Innate Immune System Interactions: Translational Potentials for Cancer Immunotherapy. J. Immunother. 2012, 35 (4), 299–308. 10.1097/CJI.0b013e3182518e83. [PubMed: 22495387]

(56). Gregory AD; Houghton AM Tumor-Associated Neutrophils: New Targets for Cancer Therapy. Cancer Res. 2011, 71 (7), 2411–2416. 10.1158/0008-5472.CAN-10-2583. [PubMed: 21427354]

(57). Carter LC; Carter JM; Nickerson PA; Wright JR; Baier RE Particle-Induced Phagocytic Cell Responses Are Material Dependent: Foreign Body Giant Cells vs. Osteoclasts from a Chick Chorioallantoic Membrane Particle-Implantation Model. J. Adhes. 2000, 74 (1–4), 53–77. 10.1080/00218460008034524.

(58). Selders GS; Fetz AE; Radic MZ; Bowlin GL An Overview of the Role of Neutrophils in Innate Immunity, Inflammation and Host-Biomaterial Integration. Regen. Biomater. 2017, 4 (1), 55–68. 10.1093/rb/rbw041. [PubMed: 28149530]

(59). Branzk N; Lubojemska A; Hardison SE; Wang Q; Gutierrez MG; Brown GD; Papayannopoulos V. Neutrophils Sense Microbe Size and Selectively Release Neutrophil Extracellular Traps in Response to Large Pathogens. Nat. Immunol. 2014, 15 (11), 1017–1025. 10.1038/ni.2987. [PubMed: 25217981]

(60). Papayannopoulos V. Neutrophil Extracellular Traps in Immunity and Disease. Nat. Rev. Immunol. 2018, 18 (2), 134–147. 10.1038/nri.2017.105. [PubMed: 28990587]

(61). Meng H; Yalavarthi S; Kanthi Y; Mazza LF; Elfline MA; Luke CE; Pinsky DJ; Henke PK; Knight JS In Vivo Role of Neutrophil Extracellular Traps in Antiphospholipid Antibody–Mediated Venous Thrombosis. Arthritis Rheumatol. 2017, 69 (3), 655–667. 10.1002/art.39938. [PubMed: 27696751]

(62). Leffler J; Stojanovich L; Shoenfeld Y; Bogdanovic G; Hesselstrand R; Blom A. Degradation of Neutrophil Extracellular Traps Is Decreased in Patients with Antiphospholipid Syndrome. Clin. Exp. Rheumatol. 2014, 32 (1), 66–70. [PubMed: 24295292]

(63). He Y; Yang FY; Sun EW Neutrophil Extracellular Traps in Autoimmune Diseases. Chin. Med. J. (Engl). 2018, 131 (13), 1513–1519. 10.4103/0366-6999.235122. [PubMed: 29941703]

(64). Fromen CA; Fish MB; Zimmerman A; Adili R; Holinstat M; Eniola-Adefeso O. Evaluation of Receptor-Ligand Mechanisms of Dual-Targeted Particles to an Inflamed Endothelium. Bioeng. Transl. Med. 2016, 1 (1), 103–115. 10.14574/ojrnhc.v14i1.276.Using. [PubMed: 28066821]

(65). Charoenphol P; Onyskiw PJ; Carrasco-Teja M; Eniola-Adefeso O. Particle-Cell Dynamics in Human Blood Flow: Implications for Vascular-Targeted Drug Delivery. J. Biomech. 2012, 45 (16), 2822–2828. 10.1016/j.jbiomech.2012.08.035. [PubMed: 23010218]

(66). Huang RB; Eniola-Adefeso O. Shear Stress Modulation of IL-1B-Induced E-Selectin Expression in Human Endothelial Cells. PLoS One 2012, 7 (2), 1–9. 10.1371/journal.pone.0031874.

(67). Casa LDC; Deaton DH; Ku DN Role of High Shear Rate in Thrombosis. J. Vasc. Surg. 2015, 61 (4), 1068–1080. 10.1016/j.jvs.2014.12.050. [PubMed: 25704412]

(68). Jackson SP The Growing Complexity of Platelet Aggregation. Blood 2007, 109 (12), 5087–5095. 10.1182/blood-2006-12-027698. [PubMed: 17311994]

(69). Ku DN; Giddens DP; Zarins CK; Glagov S. Pulsatile Flow and Atherosclerosis in the Human Carotid Bifurcation. Positive Correlation between Plaque Location and Low and Oscillating Shear Stress. Arteriosclerosis 1985, 5 (3), 293–302. [PubMed: 3994585]

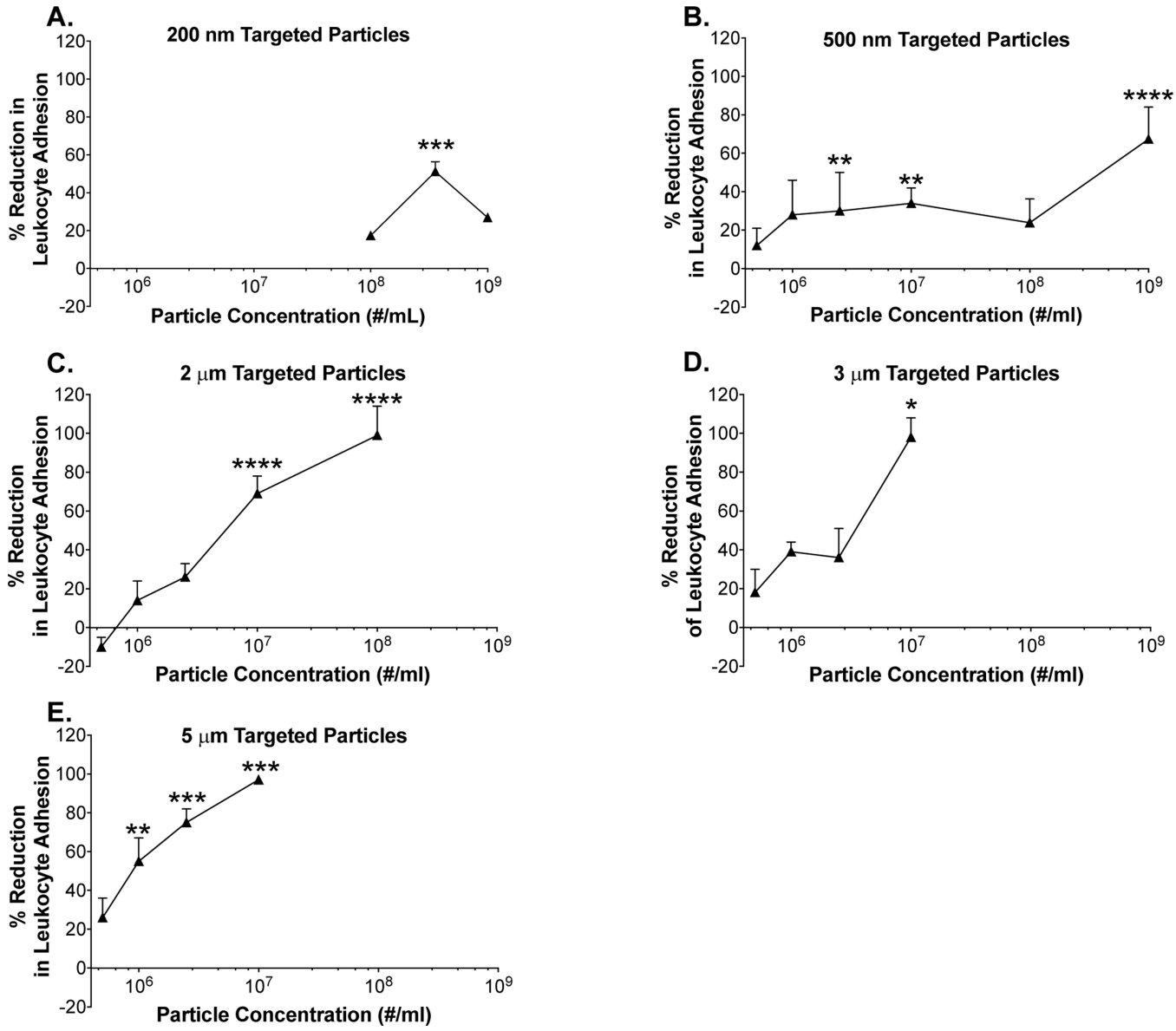

Figure 1 - Reduction of leukocyte adhesion observed following pulsatile flow with (a) 200 nm, (b) 500 nm, (c) 2 μm, (d) 3 μm, and (e) 5 μm targeted (sLe^A) particles.

(*) indicates significant difference in leukocyte adhesion of targeted (sLe^A) particles relative to particle-free blood, ($p<0.05$). Statistical analysis was performed Kruskal-Wallis with $\alpha = 0.01$. $n \geq 3$ donors for each particle size and concentration. Error bars represent standard error.

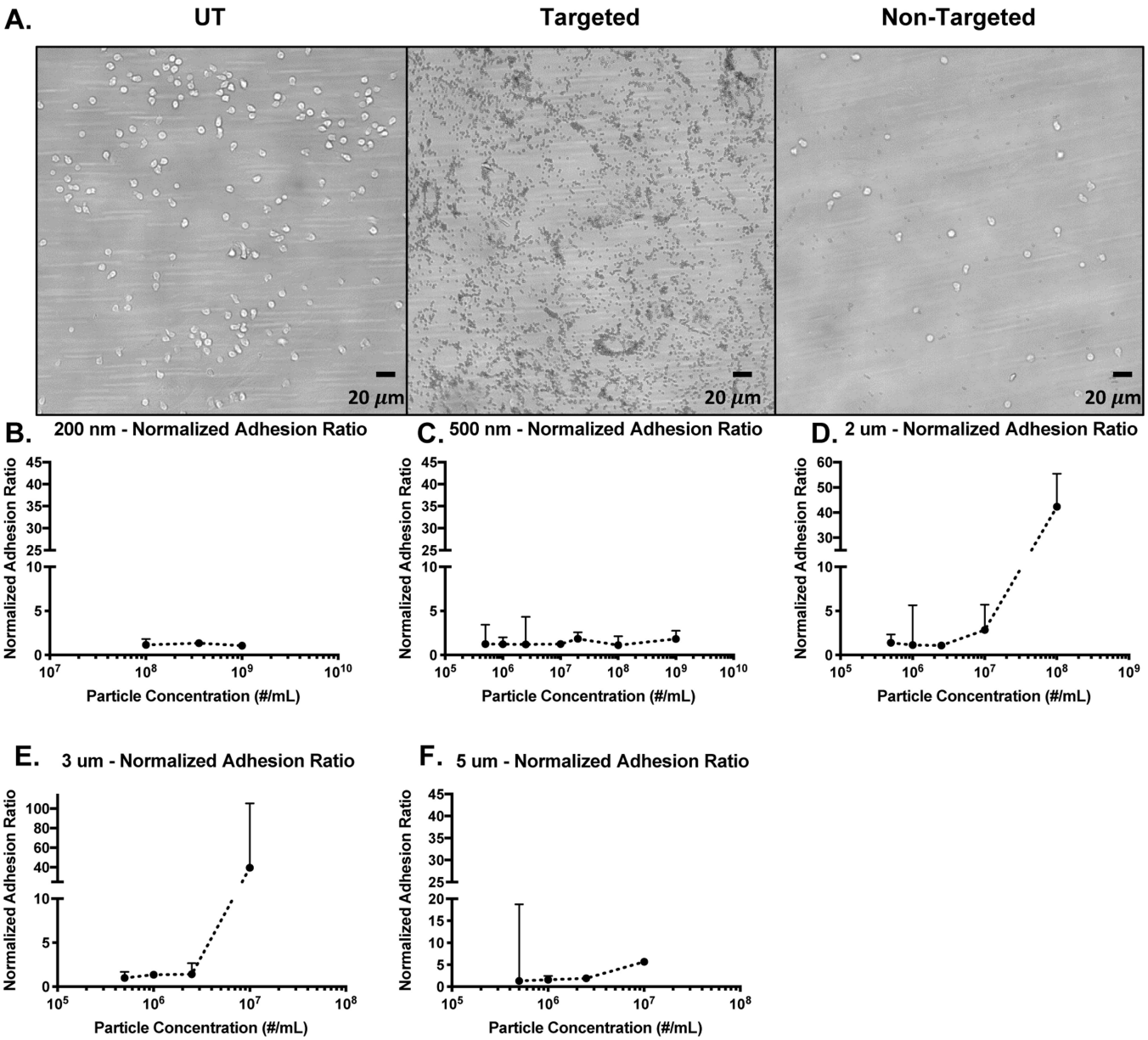

Figure 2 - Normalized Adhesion Ratio of Non-Targeted versus Targeted Particles.

(a) Example images of leukocyte and particle ($2\ \mu m,\ 1E8/mL$) adhesion on a HUVEC monolayer. Ratio of leukocyte adhesion (Non-targeted over Targeted Particles) relative to particle-free blood for (b) 200 nm, (c) 500 nm, (d) 2 μm, (e) 3 μm, and (f) 5 μm targeted (sLe^A) particles.

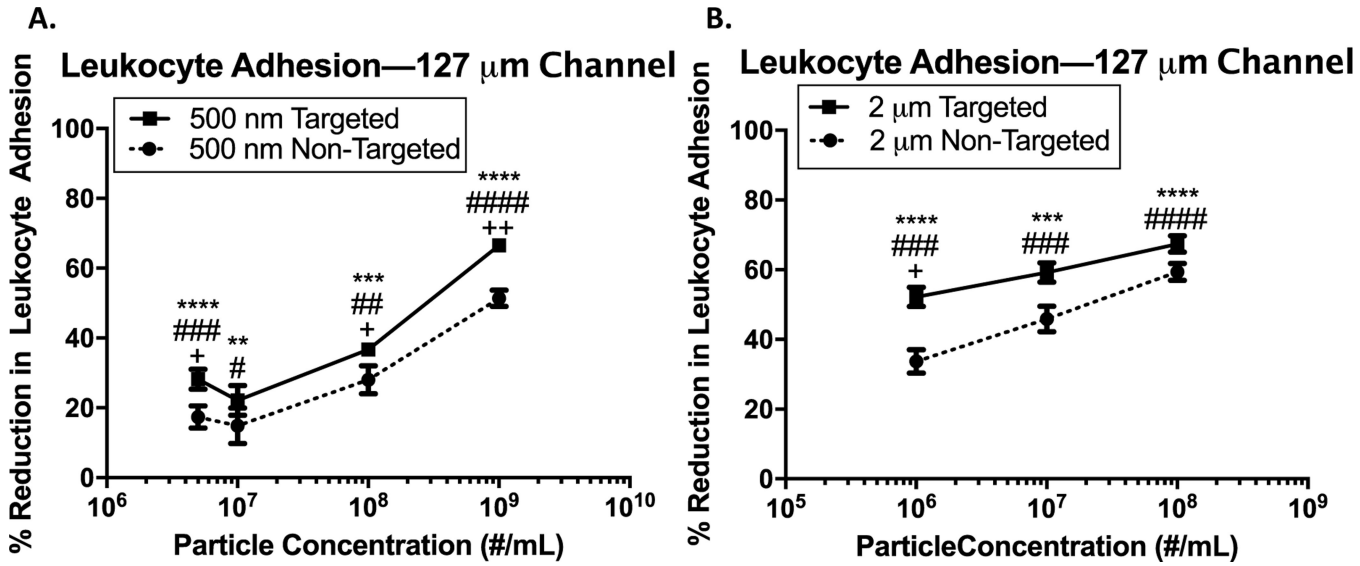

Figure 3 - Particle reduction of leukocyte adhesion in pulsatile blood flow in 127 μm channel.

(a) Percent reduction in leukocyte adhesion to an inflamed endothelium in 127 μm channel following pulsatile blood flow with the addition of 500 nm targeted and non-targeted particles at varying concentrations. (b) Percent reduction in leukocyte adhesion to an inflamed endothelium in 127 μm channel following pulsatile blood flow with the addition 2 μm targeted and non-targeted particles at varying concentrations. (*) indicates significant difference in leukocyte adhesion of targeted (sLe^A) particles relative to particle-free blood, (#) indicates significant difference in leukocyte adhesion of non-targeted particles relative to particle-free blood, and (+) indicates significant difference between targeted and non-targeted groups ($p<0.05$). Statistical analysis was performed using one-way ANOVA using GraphPad Prism software. $n \geq 3$ donors for each particle size and concentration. Error bars represent standard error.

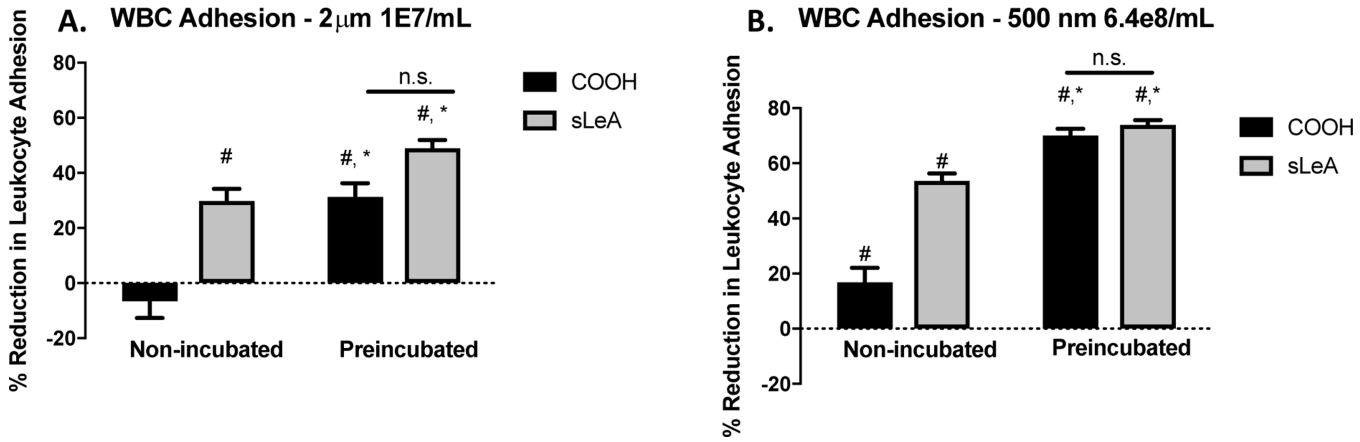

Figure 4 - Impact of Particle Internalization on Leukocyte Adhesion in Pulsatile Flow.

(a) Leukocyte adhesion in whole blood following pulsatile flow at $1000s^{-1}$ shear over an activated HUVEC monolayer for 15 minutes for blood with carboxylated and sialyl Lewis A-conjugated 2 μm polystyrene particles at a concentration of 1E7/mL, normalized to the particle-free control. (b) Leukocyte adhesion in whole blood following pulsatile flow at $1000s^{-1}$ shear over an activated HUVEC monolayer for 15 minutes for blood with carboxylated and sialyl Lewis A-conjugated 500 *n*m polystyrene particles at a concentration of 6.4E8/mL, normalized to the particle-free control. (#) indicates a significant reduction from the particle-free control; (*) indicates a significant reduction between the 'non-incubated' and 'preincubated' conditions for that particle type ($p<0.05$). $n\geq3$ donors for each bar shown. Statistical analysis was performed using one-way ANOVA using GraphPad Prism software.

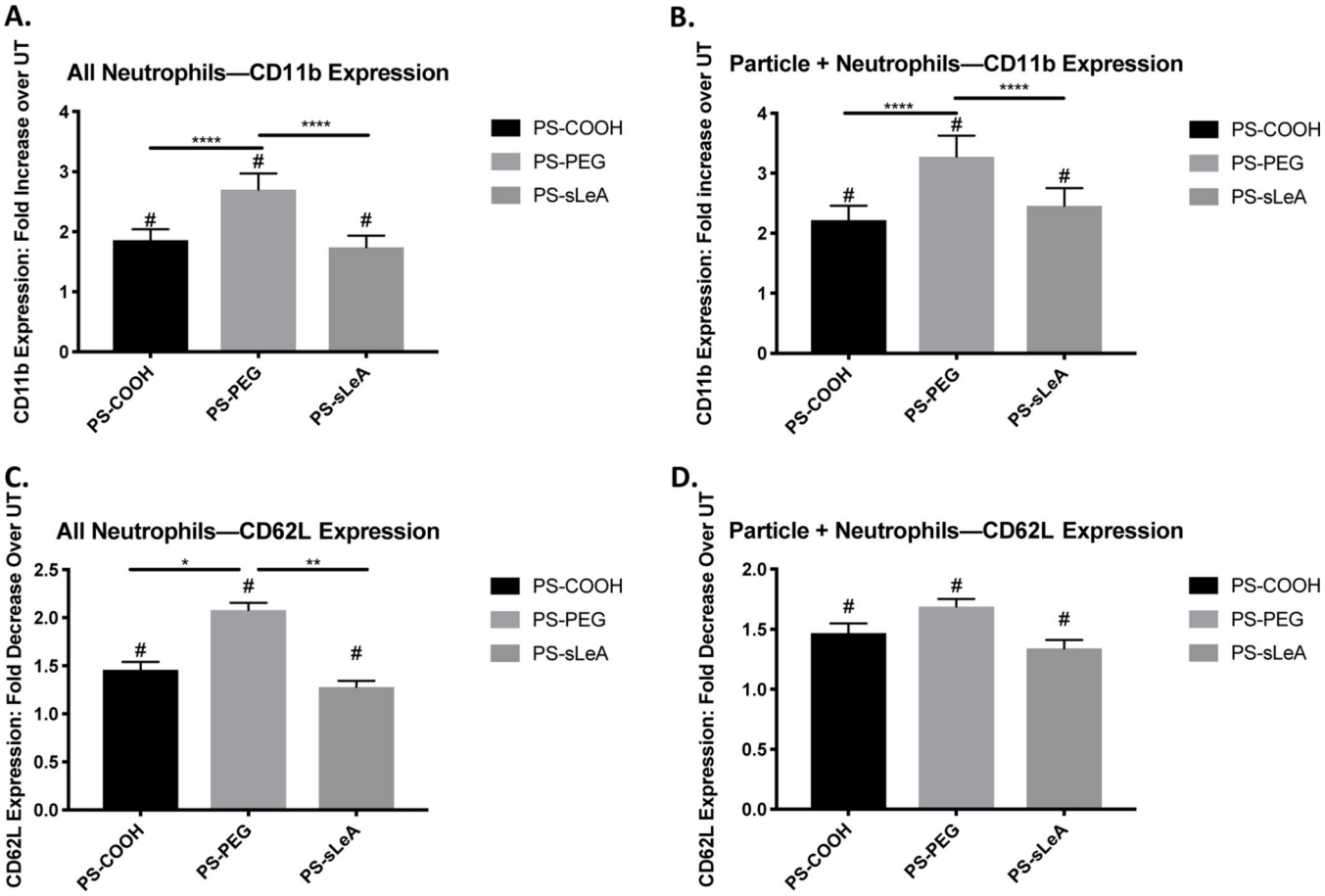

Figure 5 - Impact of Particle Internalization on Neutrophil Expression of CD11b and CD62L.

(a) Fold change in CD11b expression over untreated for all neutrophils in whole blood exposed to carboxylated, PEGylated, and sialyl Lewis A-conjugated polystyrene particles. (b) Fold change in CD11b expression over untreated for particle-positive neutrophils in whole blood exposed to carboxylated, PEGylated, and sialyl Lewis A-conjugated polystyrene particles. (c) Fold decrese in CD62L expression over untreated for all neutrophils in whole blood exposed to carboxylated, PEGylated, and sialyl Lewis A-conjugated polystyrene particles. (d) Fold decrease in CD62L expression over untreated for particle-positive neutrophils in whole blood exposed to carboxylated, PEGylated, and sialyl Lewis A-conjugated polystyrene particles. (#) indicates significant changes in expression from the untreated samples for each donor; (*) indicates significant differences in expression levels between particle treatment groups ($p<0.05$). Statistical analysis was performed with one-way ANOVA using GraphPad Prism software. $n\geq3$ donors for each treatment, with duplicates for every donor.